Bioorganic & Medicinal Chemistry 17 (2009) 4981–4989

Contents lists available at ScienceDirect

Bioorganic & Medicinal Chemistry

journal homepage: www.elsevier.com/locate/bmc

Synthesis and multidrug resistance reversal activity of dihydroptychantol A and its novel derivatives

Bin Sun [a], Hui-qing Yuan [b], Guang-min Xi [b], Yu-dao Ma [c,*], Hong-xiang Lou [a,*]

[a] School of Pharmaceutical Sciences, Shandong University, Jinan 200012, PR China
[b] School of Medicine, Shandong University, Jinan 250012, PR China
[c] School of Chemistry and Chemical Engineering, Shandong University, Jinan 250100, PR China

ARTICLE INFO

Article history:
Received 2 May 2009
Revised 28 May 2009
Accepted 29 May 2009
Available online 6 June 2009

Keywords:
Dihydroprychantol A
Derivatives
Multidrug resistance
P-Glycoprotein

ABSTRACT

The macrocyclic bisbibenzyl dihydroptychantol A (DHA), previously isolated from *Asterella angusta*, was synthesized and showed significant multidrug resistance (MDR) reverting activity in chemoresistant cancer cells. In an attempt to discover more potent MDR reversal agents for efficient cancer chemotherapy, DHA derivatives with thiazole rings (**19–22**) were synthesized, and their cytotoxicities and MDR reversal activities were evaluated in adriamycin-resistant K562/A02, vincristine-resistant KB/VCR and in their parental cells by MTT assays. In response to treatment with each compound, the K562 cell line was the most sensitive, and the vincristine-resistant KB/VCR cell line was the most resistant. Marked decreases in K562 and K562/A02 cell viability were detectable after treatment with the synthesized derivatives of DHA, while less inhibitory effects on cell growth were observed in chemical-resistant KB/VCR and KB cells. Moreover, among the tested compounds, the intermediate **17** and the analogues **19**, **20**, and **21** showed potent MDR reversal activities and increased vincristine cytotoxicity in KB/VCR cells, with the reversal fold ranges from 10.54 to 13.81 (10 μM), which is 3.2–4.3-fold stronger than the natural product DHA.

1. Introduction

Multidrug resistance (MDR), defined as the ability of tumor cells to show resistance to a wide variety of structurally and functionally unrelated compounds, is still one of the most serious threats to successful chemotherapy for a majority of cancer patients.[1,2] In mammals, tumors, which are initially sensitive to cytotoxic agents, often develop resistance to a broad spectrum of structurally different drugs.[3] The most significant mechanism of MDR is the overexpression of the ATP binding cassette (ABC) transporter proteins which work as energy-dependent pumps for chemotherapeutic agents and prevent drugs from reaching effective concentrations within the cells.[4] To date, the proteins of ABC family such as the *P*-glycoprotein (*P*-gp), multidrug resistance associated protein (MRP1), the lung resistance protein (LRP), and the breast cancer resistance protein (BCRP) have been discovered. The most and best-studied one is *P*-gp, which is characterized by a broad substrate spectrum.[5–8] Although a large number of compounds with a wide spectrum of chemical structures have been found to inhibit *P*-gp and reverse MDR, there are currently no reversal agents available clinically. Thus, the discovery and development of novel and potent *P*-gp inhibitory agents are still much desired, and the natural products are gaining much more attention for their anti-tumor activities.

Macrocyclic bisbibenzyls are a series of phenolic natural products that are found exclusively in bryophytes. These natural products have a variety of biological activities, including 5-lipoxygenase, cyclooxygenase and calmodulin inhibitory effects, and antifungal, anti-HIV, antimicrobial, antioxidative, muscle-relaxing, LXRα-activating, FXR-activating, and cytotoxic activities.[9–18] A recent research indicated that they also have a significant antiproliferative activity due to the inhibition of microtubule polymerization.[19,20]

In our previous reports, we found that the macrocyclic bisbibenzyl plagiochin E, which was isolated from *Marchantia polymorpha*, exhibits excellent MDR reversal activity.[21] Recently, our group also found that the macrocyclic bisbibenzyl dihydroptychantol A (DHA) (Fig. 1), isolated from liverwort *Asterella angusta* as an

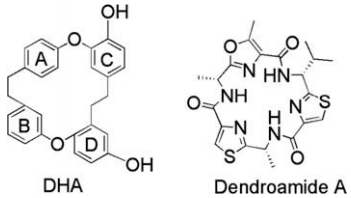

Figure 1. Chemical structures of DHA and dendroamide A.

* Corresponding authors. Tel.: +86 531 88364778; fax: +86 531 88382019.
E-mail addresses: ydma@sdu.edu.cn (Y. Ma), louhongxiang@sdu.edu.cn (H. Lou).

0968-0896/$ - see front matter © 2009 Elsevier Ltd. All rights reserved.
doi:10.1016/j.bmc.2009.05.077

antifungal natural product,[22] exhibits more potent MDR reversal activity by increasing the adriamycin cytotoxicity toward K562/A02 cells and vincristine cytotoxicity toward KB/VCR cells. DHA's mechanism of MDR reversal activity is through inhibition of *P*-gp function and its expression, which prevents efflux of drugs.[23]

The encouraging biological results motivated us to synthesize additional DHA derivatives in order to improve activity and to discover more potent MDR reversal agents. It has been reported that compounds with the thiazole ring, such as the cyclic hexapeptide dendroamide A (Fig. 1), exhibit MDR reversal activity[24–27] and some heterocyclic derivatives of combretastatin A-4, with the structure containing bibenzyl moiety, are also cytotoxic to MDR cell lines.[28] In light of these results, we were interested in the effect of the thiazole group on the macrocyclic bisbibenzyl system. Accordingly, some DHA derivatives with thiazole moieties were synthesized and their biological activities were evaluated. In this study, we report the synthetic details for DHA and its thiazole derivatives, as well as their MDR reversal activities toward the multidrug resistant cancer cell lines K562/A02 and KB/VCR. Molecular docking analyses were also used to elucidate the binding modes of the analogues to *P*-gp.

2. Results and discussion

The total synthesis of the natural product DHA was achieved in 13 steps as shown in Scheme 1. The synthetic route began with the Ullmann coupling of the protected 3-hydroxybenzaldehyde (**1**)[29] with commercially available 2-bromo-5-methoxybenzaldehyde, resulting in the formation of the diphenyl ether **2**. The phosphonium salt **7**, as the second diphenyl ether building block, was synthesized in a conventional sequence starting with S_NAr displacement of methyl 4-bromobenzoate by 3-hydroxy-4-methoxybenzaldehyde (**3**) to give the diphenyl ether **4**. Compound **4** was then reduced with sodium borohydride to give the benzyl alcohol **5**, followed by bromination and reaction with triphenylphosphine, affording **7** in four steps. The building blocks **2** and **7** were combined by the Wittig reaction in the presence of potassium carbonate and 18-crown-6,[30] and the stilbene **8** (obtained as *E*/*Z* mixture) was hydrogenated over Pd/C to give the bibenzyl **9**. Next, the carboxylic ester group of **9** was reduced with lithium aluminum hydride, followed by deprotection with HCl/H_2O to yield compound **10**. Again the bromination of **10** by carbon tetrabromide and subsequent reaction with triphenylphosphine afforded compound **12**. Cyclization of **12** by means of an intramolecular Wittig reaction was achieved with sodium methoxide, leading to key macrocyclic intermediate **13**.[31] Finally, **13** could be demethylated by boron tribromide at −78 °C to give phenol **14** or hydrogenated to give dimethyl DHA (**15**), followed by demethylation to afford the natural product DHA (**16**).

As shown in Scheme 2, the preparation of derivatives began with compound **13**, which reacted with NBS in a 1:1 mixture of THF and water at 45 °C and selectively afforded compound **17**.[32] As shown in Figure 2, the substitution pattern of the hydroxyl group and bromine atom on the fragment $CH_2(7)$–$CH_2(8)$ was confirmed by analysis of its HMBC. After the hydroxyl group was oxidized to a ketone under Swern conditions,[33] the afforded compound **18** reacted with thiourea and thiosemicarbazide, respectively, to yield the thiazoles **19** and **21**.[34] After the demethylation of **19** and **21** by boron tribromide, compounds **20** and **22**, respectively, were prepared.

To discover a promising initial candidate for MDR reversal agents, we first assayed the effect of compounds **17, 19, 20, 21**, and **22** on KB, KB/VCR, K562, and K562/A02 cells growth at a concentration of 10 μM. As shown in Table 1, treatment with bisbibenzyls resulted in cell growth decreases in the K562 and K562/A02 cells and cell viability was significantly reduced at 20, 30, and 40 μM with 58.92%, 79.26%, and 94.33% repression, respectively. Whereas, except for derivative **22**, no obvious inhibition of cell growth was oberved in the KB and KB/VCR cells.

According to our previous report, DHA and its synthetic intermediates (**13**–**15**) significantly increased the sensitivity toward adriamycin in K562/A02 cells.[23] However, when coadministered with adriamycin, each derivative compound (**17, 19**–**21**) did not remarkably improve adriamycin's cytotoxicity in K562/A02 cells at 10 μM, and their reversal fold ranged from 1.65 to 2.68, which were no better than that of DHA (5.22). These results imply that K562/A02 cells are not sensitive to thiazole derivatives. We then tested the MDR reversal effect of these four compounds on KB/VCR cells at the same concentration. To our surprise, when coadministered with each derivative compound, there was a great increase in cytotoxicity of vincristine toward KB/VCR cells, and as shown in Table 2, its ID_{50} ranged from 0.135 to 0.177 μM, and the MDR reversal fold of these compounds ranged from 10.58 to 13.81. It is obvious that their MDR reversal effects are much more potent than that of DHA (3.25).[23]

Based on the test results, we can find that the MDR reversal potency of DHA has been improved greatly by the introduction of a thiazole ring to the macrocyclic bisbibenzyl system, and the KB/VCR cells are more sensitive to DHA derivatives than K562/A02 cells.

This excellent bioactivity encouraged us to investigate the possible mechanism of action at the molecular level, specifically, the binding mode of bisbibenzyls to *P*-glycoprotein. Recently, Chang et al.[35] solved the crystal structure of murine *P*-gp (which has 87% sequence identity to the human protein) in complex with ligands. According to their research, there are three binding sites in the protein. In order to figure out the best binding site for DHA and its analogues, the compounds **15**, **17**, **19**–**21** and DHA were docked into all three potential binding sites of Chang's structure using the program GOLD (Genetic Optimization for Ligand Docking).[36–38]According to our docking results, we found that the top 10 ranked conformations of each compound are almost the same and the best ranked conformation of each compound overlays very well with each other in the binding site of Chang's ligand cyclic-*tris*-(*R*)-valineselenazole (QZ59-RRR).[35] Based on this result, it is likely that our compounds bind in the same site as QZ59-RRR and Figure 3 shows the top-ranked GOLD pose for each compound.

The binding mode of the representative compound **19** has been studied further by energy minimization. In this minimized docking mode for compound **19**, the amine group of the thiazole forms a hydrogen bond with the backbone carbonyl group of Ser725. Also, the thiazole ring may form a π-π interaction with the phenyl ring of Phe728, (Figs. 4 and 5A). We believe that these interactions are responsible for enhancing the *P*-gp inhibitory activity of thiazole derivatives. It is also possible that the methoxyl group of ring C forms a hydrogen bond with the amide group of Gln 721, and a CH-π interaction[39] between this group and Tyr 303 (Fig. 5A) may exist as well. As shown in Figure 5A and B, rings A and C exhibit potential π-π interactions with phenyl groups of Phe 724 and Phe 974, respectively, and ring A may also create a CH-π interaction with methyl group of Val 978. We were able to observe that the methoxyl group of ring D could fit into the hydrophobic pocket formed by Leu 64, Met 68, and Ile 336 as well (Figs. 5A and 6). These combined π–π interactions, CH–π interaction, and hydrogen bonds could play a crucial role in *P*-gp inhibitory activity of the macrocyclic bisbibenzyl compounds. In addition, as shown in Figure 3, DHA and compound **20**, with the phenolic hydroxyl group on C ring, may create stronger hydrogen bonds with Gln 721, and this could contribute to their higher potency than the compounds with methoxyl groups. The loss of the hydroxyl and amine groups (as in compound **15**) attenuates these hydrogen bond inter-

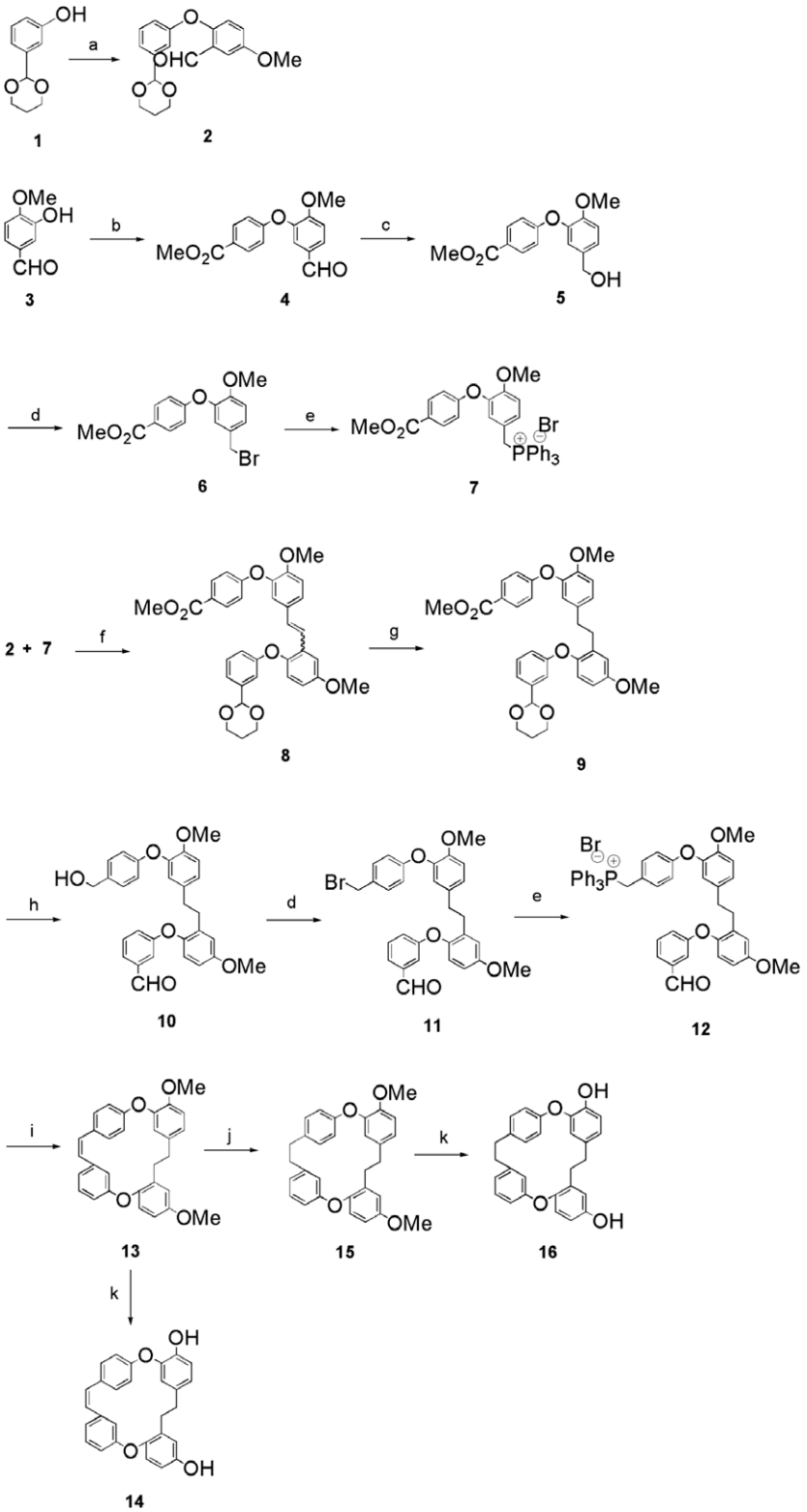

Scheme 1. Synthesis of DHA. Reagents and conditions: (a) 2-bromo-5-methoxybenzaldehyde, K_2CO_3, CuO, pyridine, reflux; (b) 4-bromobenzoate, K_2CO_3, pyridine, CuO, reflux; (c) $NaBH_4$, THF, rt; (d) CBr_4, PPh_3, CH_2Cl_2, 0 °C; (e) PPh_3, toluene, reflux; (f) K_2CO_3, 18-crown-6, CH_2Cl_2, reflux; (g) H_2, 10% Pd/C, Et_3N, AcOEt, rt; (h) (1) $LiAlH_4$, THF, 30 °C; (2) H^+/H_2O, rt; (i) NaOMe, CH_2Cl_2, rt; (j) H_2, 10% Pd/C, AcOEt, rt; (k) BBr_3, CH_2Cl_2, −78 °C.

actions and may be responsible for the lower activity of **15**. Overall, the docking studies revealed that bisbibenzyl and its analogues interacted with *P*-gp in the same binding site as QZ59-RRR, and also supported that the macrocyclic bisbibenzyl skeleton is the basic structure for the MDR reversal activity, and the increased inhibitory effect of derivatives **19**, **20**, and **21** is due to their hydrogen bonds and π–π interactions with active site amino acid residues of *P*-gp.

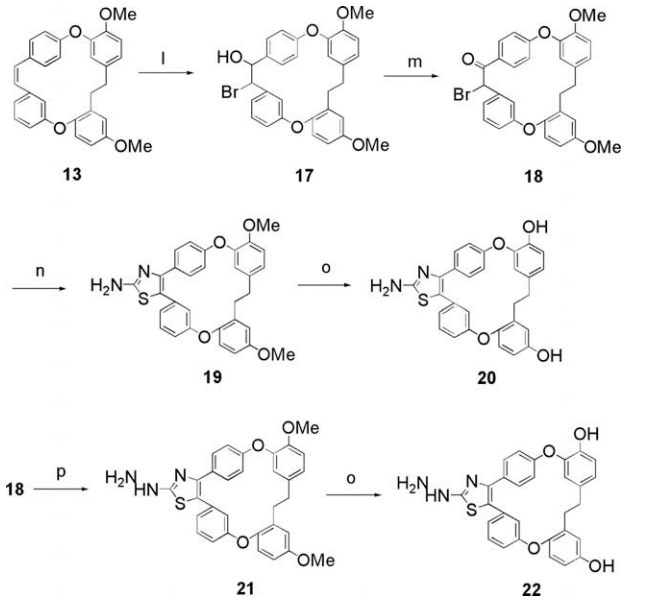

Scheme 2. Synthesis of DHA's derivatives. Reagents and conditions: (l) NBS, THF/H_2O (1:1), 45 °C; (m) DMSO, TFAA, CH_2Cl_2, −78 °C; (n) thiourea, DMF, 60 °C; (o) BBr_3, CH_2Cl_2; −78 °C; (p) thiosemicarbazide, DMF, 75 °C; (q) thioacetamide, K_2CO_3, DMF, 80 °C.

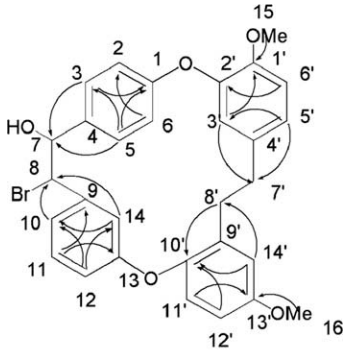

Figure 2. The substitution of hydroxyl group and bromine atom on the fragment $CH_2(7)$–$CH_2(8)$ was confirmed by the following long-range correlations (Fig. 1): H-3 and H-5 with C-7, H-10 and H-14 with C-8, H-3′ and H-5′ with C-7′, H-10′ and H-14′ with C-8′ by use of HMBC.

3. Conclusions

As shown in Schemes 1 and 2, and Tables 1 and 2, we have achieved the total synthesis of DHA, prepared a series of derivatives (**19**, **20**, **21**, and **22**) with the thiazole ring system, and tested their MDR reversal activity toward K562/A02 and KB/VCR cells. Among the tested compounds, **20** showed the most potent MDR reversal activity toward KB/VCR cells. While compounds **17**, **19**, and **21** also exhibited excellent bioactivity. In addition, molecular docking analyses were also used to elucidate the binding models of the analogues to *P*-gp. From the study of a preliminary structure–activity relationship, it was considered that the macrocyclic bisbibenzyl skeleton is the basic structure for the MDR reversal activity, and the phenolic hydroxyl groups, amine group, and thiazole ring could play essential roles in enhancing the *P*-gp inhibitory activity of bisbibenzyls. In conclusion, the macrocyclic bisbibenzyl system is a promising scaffold for the development of novel MDR reversal agents for cancer chemotherapy and merits further investigation. In order to discover novel MDR reversal agents for efficient cancer chemotherapy, we will screen additional natural products with different macrocyclic bisbibenzyl skeletons and direct our efforts toward rational modifications of the promising candidates.

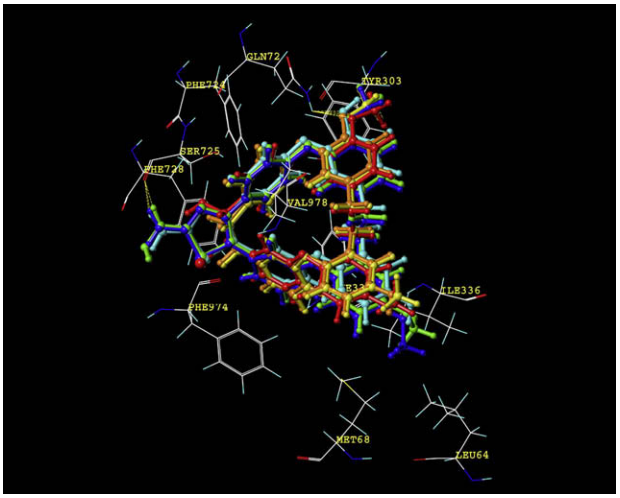

Figure 3. Overlap of the best-docked conformations of compounds **15** (yellow), **17** (red), **19** (blue), **20** (cyan), **21** (green) and DHA (orange) in the binding site, and the hydrogen bonds are labeled as yellow broken lines.

Table 1
Inhibitory effect of DHA's derivatives on cells[a]

Compound	K562 % of inhibition	K562/A02 % of inhibition	KB % of inhibition	KB/VCR % of inhibition
17	38.55	11.86	2.82	0
19	58.67	26.81	0	0
20	11.56	10.11	0	0
21	32.07	18.76	0	0
22	37.15	13.69	51.15	19.42

[a] After treatment of cancer cells with 10 μM of each compound for 48 h, the inhibitory rate (%) was calculated by using the MTT assay.

Table 2
Multidrug resistance (MDR) reversal activity of DHA's derivatives against KB/VCR cells[a]

Treatment	ID_{50}[b] (μM) (KB/VCR)	RF (KB/VCR)
VCR	1.864 ± 0.702	
VCR + **17** (10 μM)	0.177 ± 0.012	**10.54**
VCR + **19** (10 μM)	0.152 ± 0.003	**12.26**
VCR + **20** (10 μM)	0.135 ± 0.009	**13.81**
VCR + **21** (10 μM)	0.176 ± 0.016	**10.58**

Bold numbers emphasize the excellent biological activity.

[a] KB/VCR cells were seeded at a density of 6×10^4/ml in 24-well plates and co-treated with various concentrations of vincristine in the presence of 17, 19, 20, 21, 22, or 23 at the concentration of 10 μM. Cell viability was determined using the MTT assay.

[b] Data are expressed as means ± standard deviation from three independent experiments. $^*P < 0.05$.

4. Experimental

4.1. General procedures

Column chromatography was carried out on silica gel or alumina (200–300 mesh). Reactions were monitored by thin-layer chromatography, using Merck plates with fluorescent indicator. Melting points were determined on an X-6 melting-point apparatus and are uncorrected. The ^1H NMR spectra were recorded on a

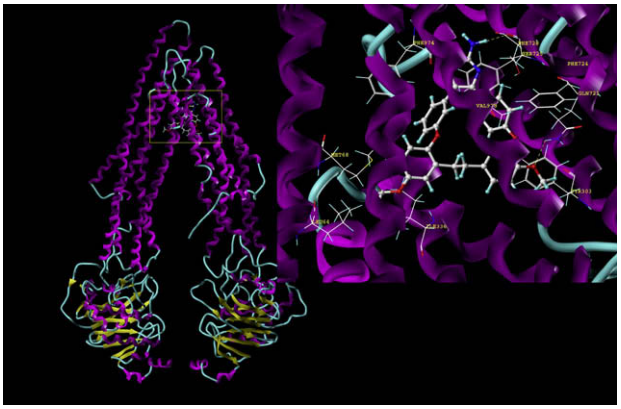

Figure 4. Ribbon diagram illustrating the crystal structure of murine *P*-gp with compound **19** bound to the active site, and the hydrogen bonds are labeled as yellow broken lines.

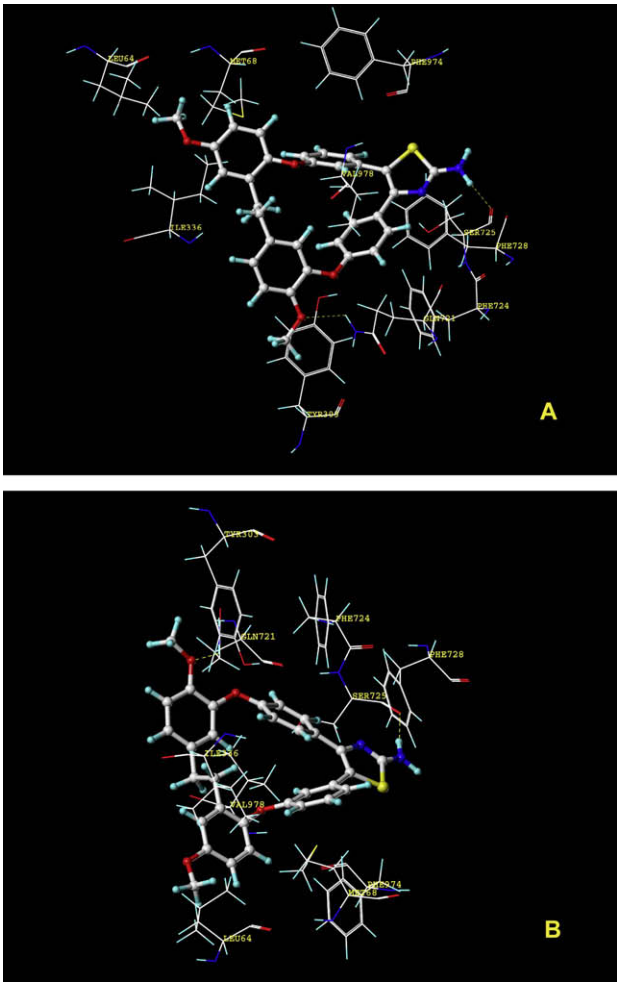

Figure 5. Potential interactions between compound **19** and Leu64, Met 68, Tyr 303, Ile 336, Gln 721, Ser725, Phe728, Phe 974, Val 978 (A), and Phe 724 (B) in the murine *P*-gp active site, and the hydrogen bonds are labeled as yellow broken lines.

Bruker Spectospin spectrometer at 300 or 600 MHz, using TMS as an internal standard. The chemical shifts are reported in parts per million (ppm δ) referenced to the residual ^{1}H resonance of the solvent ($CDCl_3$, 7.26 ppm). Abbreviations used in the splitting pattern were as follows: s = singlet, d = doublet, t = triplet, quin = quintet, m = multiplet, and br = broad. All HRMS spectra (ESI) were obtained on a LTQ Orbitrap mass spectrometer.

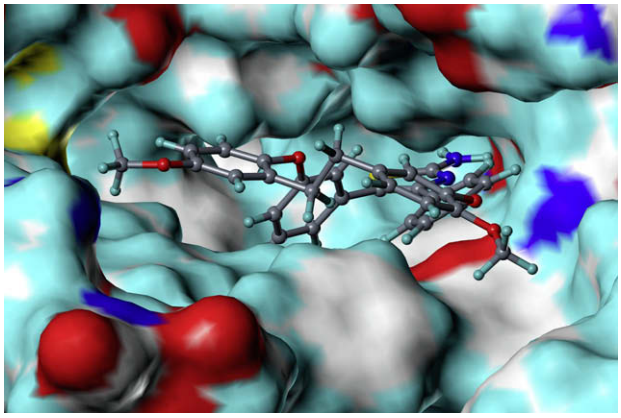

Figure 6. Top-ranked, minimized docking pose compound **19** in murine *P*-gp active site.

Reagents were used as purchased without further purification. Solvents (THF, DMF, CH_2Cl_2, DMSO, and toluene) were dried and freshly distilled before use according to the procedures reported in the literature.

4.2. Syntheses

4.2.1. 2-(3-(1,3-Dioxan-2-yl)phenoxy)-5-methoxybenzaldehyde (2)

A mixture of 3-(1,3-dioxan-2-yl)phenol (**1**,[23] 8.81 g, 48.12 mmol), 2-bromo-5-methoxybenzaldehyde (10.27 g, 48.12 mmol), potassium carbonate (13.24 g, 96.33 mmol), and cupric oxide (0.38 g, 4.82 mmol) in pyridine (50 mL) was stirred under reflux for 12 h. The pyridine was distilled off in vacuo and the residue was extracted with ethyl acetate (200 mL). The solution was concentrated and the residue was purified by flash column chromatograph (Al_2O_3), eluting with a 2:1 solution of petroleum ether–CH_2Cl_2 to afford **2** (8.92 g, 62%) as a yellow solid; mp 66–67 °C. ^{1}H NMR (300 MHz, $CDCl_3$) δ 10.38 (s, 1H), 7.40 (d, J = 3.3 Hz, 1H), 7.33 (d, J = 8.1 Hz, 1H), 7.23 (s, 1H), 7.16 (s, 1H), 7.12 (dd, J = 9.1, 3.1 Hz, 1H), 6.97–6.91 (m, 2H), 5.47 (s, 1H), 4.26 (dd, J = 10.7, 5.1 Hz, 2H), 3.97 (dt, J = 12, 2.4 Hz, 2H), 3.85 (s, 3H), 2.28–2.15 (m, 1H), 1.45 (d, J = 13.5 Hz, 1H); MS (ESI) 315 $(M+H)^+$.

4.2.2. Methyl 4-(5-formyl-2-methoxyphenoxy) benzoate (4)

This compound was prepared from methyl 4-bromobenzoate (15.05 g, 69.98 mmol) and 3-hydroxy-4-methoxybenzaldehyde (10.63 g, 69.98 mmol) by means of a procedure similar to that used for **2**. After concentration of the solution, the residue was purified by flash column chromatography (SiO_2), eluting with a 3:2 solution of petroleum ether–CH_2Cl_2 to afford **4** (13.01 g, 65%) as an orange solid; mp 118–120 °C. ^{1}H NMR (300 MHz, $CDCl_3$) δ 9.87 (s, 1H), 8.02–7.99 (m, 2H), 7.76 (dd, J = 8.2, 2.1 Hz, 1H), 7.59 (d, J = 2.1 Hz, 1H), 7.14 (d, J = 8.3 Hz, 1H), 6.94 (d, J = 8.7 Hz, 2H), 3.91 (s, 3H), 3.90 (s, 3H); MS (ESI) 287 $(M+H)^+$.

4.2.3. Methyl 4-(5-(hydroxymethyl)-2-methoxyphenoxy) benzoate (5)

Sodium borohydride (0.68 g, 18.32 mmol) was added to a solution of **4** (12.87 g, 45.73 mmol) in THF (40 mL) over 15 min at 0 °C. The reaction mixture was then stirred at room temperature for 3 h. Water (10 mL) and 1 M HCl (18 mL) were added and the THF was evaporated in vacuo. The resulting mixture was extracted with CH_2Cl_2 (20 mL), washed with satd aq NaCl (10 mL × 3), and dried over sodium sulfate. The solution was concentrated to obtain a crude oil that was purified by flash column chromatography (SiO_2), eluting with CH_2Cl_2 to afford **5** (11.41 g, 88%) as a white solid; mp 77–79 °C. ^{1}H NMR (300 MHz, $CDCl_3$) δ 7.97 (d, J = 8.7 Hz,

2H), 7.21 (dd, J = 8.1, 1.8 Hz, 1H), 7.09 (d, J = 1.8 Hz, 1H), 7.00 (d, J = 8.1 Hz, 1H), 6.92 (d, J = 8.7 Hz, 2H), 4.63 (s, 2H), 3.89 (s, 3H), 3.80 (s, 3H), 1.67 (br s, 1H); MS (ESI) 289 $(M+H)^+$.

4.2.4. (4-Methoxy-3-(4-(methoxycarbonyl)phenoxy)benzyl)-triphenylphosphonium bromide (7)

Carbon tetrabromide (25.91 g, 78.43 mmol) and triphenylphosphine (11.24 g, 43.12 mmol) were successively added to a stirred solution of **5** (11.23 g, 39.23 mmol) in CH_2Cl_2 (50 mL) over 30 min at 0 °C. The resulting reaction mixture was then stirred at 0 °C for 2.5 h. The solution was concentrated to obtain an orange oil that was purified by flash column chromatography (SiO_2), eluting with a 2:1 solution of petroleum ether–CH_2Cl_2, to afford **6** (12.04 g, 88%) as a white solid. The compound **6** (11.9 g, 34.43 mmol) was added subsequently to a solution of triphenylphosphine (9.8 g, 37.32 mmol) in anhydrous toluene, and the reaction mixture was then stirred under reflux for 3 h. The reaction mixture was allowed to cool to room temperature, and the precipitate was filtered and washed with hexane to provide **7** (20.43 g, 98%) as a white solid; mp 217–219 °C. ^{1}H NMR (300 MHz, $CDCl_3$) δ 7.90 (d, J = 9.0 Hz, 2H), 7.80–7.73 (m, 9H), 7.65–7.58 (m, 6H), 7.27 (s, 1H), 6.84 (d, J = 8.4 Hz, 1H), 6.69 (d, J = 8.7 Hz, 2H), 6.51 (s, 1H), 5.46 (d, J = 14 Hz, 2H), 3.90 (s, 3H), 3.73 (s, 3H); MS (ESI) 533 $(M-Br)^+$.

4.2.5. (*E*/*Z*)-Methyl 4-(5-(2-(3-(1,3-dioxan-2-yl)phenoxy)-5-methoxystyryl)-2-methoxy- phenoxy) benzoate (8)

Potassium carbonate (7.73 g, 56.09 mmol) and a small amount of 18-crown-6 were added to a solution of **2** (8.79 g, 28.03 mmol) and **7** (18 g, 29.30 mmol) in anhydrous CH_2Cl_2 (50 mL), and the resulting mixture was stirred under reflux for 24 h. The insoluble material was then filtered off and the filtrate was concentrated to provide the orange oil that was purified by flash column chromatography (Al_2O_3), eluting with a 2:1 solution of petroleum ether–CH_2Cl_2 to afford **8** (13.68 g, 86%) as a yellow oil.

4.2.6. Methyl 4-(5-(2-(3-(1,3-dioxan-2-yl)phenoxy)-5-methoxyphenethyl)-2-methoxy- phenoxy) benzoate (9)

Pd/C 10% (1 g) and triethylamine (27 mL) were added to a solution of **8** (13.63 g, 24.06 mmol) in ethyl acetate (150 mL). The suspension was stirred under H_2 for 24 h at room temperature. The mixture was filtered, and concentration provided a crude yellow solid that was purified by precipitating from ethyl ether–petroleum ether to afford **9** (13.4 g, 98%) as a white solid; mp 103–104 °C. ^{1}H NMR (300 MHz, $CDCl_3$) δ 7.95 (d, J = 9 Hz, 2H), 7.22 (d, J = 7.8 Hz, 1H), 7.12 (d, J = 8.3 Hz, 1H), 7.02 (s, 1H), 6.93–6.80 (m, 7H), 6.72–6.67 (m, 2H), 5.42 (s, 1H), 4.23 (dd, J = 10.5, 5.1 Hz, 2H), 3.96 (dd, J = 12.3, 2.7 Hz, 2H), 3.88 (s, 3H), 3.76 (s, 3H), 3.75 (s, 3H), 2.80 (s, 4H), 2.27–2.11 (m, 1H), 1.42 (d, J = 13.5 Hz, 1H); MS (ESI) 571 $(M+H)^+$.

4.2.7. 3-(2-(3-(4-(Hydroxymethyl)phenoxy)-4-methoxyphenethyl)-4-methoxyphenoxy) benzaldehyde (10)

A solution of **9** (13.11 g, 23.72 mmol) in anhydrous THF (25 mL) was added dropwise to a stirred suspension of lithium aluminum hydride (1.75 g, 46.07 mmol) in anhydrous THF (30 mL). The resulting mixture was stirred at room temperature for 2.5 h and carefully hydrolyzed with satd aq ammonium chloride (10 mL). THF was removed in vacuo and the resulting mixture was diluted with CH_2Cl_2 (100 mL), washed with satd aq NaCl (20 mL × 3), and dried over sodium sulfate. The solution was concentrated to obtain a crude oil that was subsequently dissolved in a solution of ethanol (100 mL) and 10% aq HCl (20 mL). The resulting mixture was then stirred at room temperature for 12 h. Satd aq sodium bicarbonate (150 mL) was added and the ethanol was removed in vacuo. The resulting mixture was extracted with CH_2Cl_2 (200 mL), washed with satd aq NaCl (25 mL × 3), and dried over sodium sulfate. The solution was concentrated to yield **10** (9.64 g, 87%) as colorless oil. ^{1}H NMR (300 MHz, $CDCl_3$) δ 9.85 (s, 1H), 7.49 (d, J = 7.5 Hz, 1H), 7.40 (t, J = 7.9 Hz, 1H), 7.27–7.25 (m, 3H), 7.11 (dd, J = 8.1, 1.8 Hz, 1H), 6.90–6.81 (m, 5H), 6.76–6.72 (m, 2H), 6.66 (d, J = 1.36 Hz, 1H), 4.62 (s, 2H), 3.77 (s, 6H), 2.75 (s, 4H), 1.79 (br s, 1H); MS (ESI) 483 $(M+H)^+$.

4.2.8. (4-(5-(2-(3-Formylphenoxy)-5-methoxyphenethyl)-2-methoxyphenoxy)benzyl) triphenylphosphonium bromide (12)

Carbon tetrabromide (13.28 g, 40.02 mmol) and triphenylphosphine (5.76 g, 22.39 mmol) were successively added to a stirred solution of **10** (9.64 g, 20.67 mmol) in CH_2Cl_2 (50 mL) over 20 min at 0 °C. The resulting reaction mixture was then stirred at 0 °C for 2.5 h. Removal of solvent in vacuo afforded an orange oil which was purified by flash column chromatography (SiO_2), eluting with a 2:1 solution of petroleum ether–CH_2Cl_2, to yield **11** (8.92 g, 79%) as a white solid. The compound **11** (8.92 g, 16.3 mmol) was then added subsequently to a solution of triphenylphosphine (4.7 g, 18 mmol) in toluene, and the reaction mixture was heated at reflux for 3 h. The reaction mixture was allowed to cool to room temperature, and the precipitate was filtered and washed with hexane to provide **12** (12.9 g, 98%) as a white solid; mp 233–235 °C. ^{1}H NMR (300 MHz, $CDCl_3$) δ 9.90 (s, 1H), 7.78–7.71 (m, 9H), 7.65–7.59 (m, 6H), 7.53–7.39 (m, 2H), 7.25–7.10 (m, 2H), 7.02 (d, J = 6.3 Hz, 2H), 6.88–6.63 (m, 8H), 5.40 (d, J = 13.8 Hz, 2H), 3.77 (s, 3H), 3.75 (s, 3H), 2.75 (s, 4H); MS (ESI) 729 $(M-Br)^+$.

4.2.9. Dimethyl ether of isoptychantol A (13)

A solution of **12** (1.13 g, 1.41 mmol) in anhydrous CH_2Cl_2 (150 mL) was added dropwise to a stirred suspension of sodium methoxide (152 mg, 2.82 mmol) in anhydrous CH_2Cl_2 (200 mL) over 7 h and the reaction mixture was stirred for 5 h at room temperature. The reaction mixture was filtered, concentrated, and the residue was purified by flash column chromatography (SiO_2), eluating with CH_2Cl_2 to yield **13** (0.49 g, 78%) as a white solid; mp 170–171 °C. ^{1}H NMR (600 MHz, $CDCl_3$) δ 7.18–7.13 (m, 3H), 7.08 (d, J = 8.4 Hz, 2H), 6.92 (d, J = 9 Hz, 2H), 6.86 (t, J = 8.7 Hz, 2H), 6.82 (d, J = 2.4 Hz, 1H), 6.80 (d, J = 1.8 Hz, 1H), 6.75–6.72 (m, 2H), 6.69 (s, 1H), 6.42 (d, J = 1.8 Hz, 1H), 6.40 (d, J = 1.8 Hz, 1H), 3.95 (s, 3H), 3.82 (s, 3H), 2.60–2.58 (m, 2H), 2.56–2.54 (m, 2H); MS (ESI) 451 $(M+H)^+$.

4.2.10. Isoptychantol A (14)

A solution of boron tribromide (1.95 g, 7.83 mmol) in anhydrous CH_2Cl_2 (10 mL) was added dropwise to a stirred solution of **13** (0.44 g, 0.98 mmol) in anhydrous CH_2Cl_2 (10 mL) at −78 °C. The reaction mixture was stirred at −78 °C for 3 h, and then was allowed to warm up to room temperature within 12 h. The ice-cold water was added, and the reaction mixture was stirred vigorously for 1 h. The solution was then diluted with CH_2Cl_2 (50 mL), washed with satd aq NaCl (20 mL × 3), and dried over sodium sulfate. The solution was concentrated, and the residue was purified by flash column chromatography (SiO_2), eluting with CH_2Cl_2 to yield **14** (0.3 g, 73%) as a grey solid. mp 93–95 °C. ^{1}H NMR (300 MHz, $CDCl_3$) δ 7.18–7.11 (m, 3H), 6.97 (dd, J = 8.5, 1.8 Hz, 2H), 6.88–6.85 (m, 2H), 6.75–6.71 (m, 4H), 6.66–6.63 (m, 3H), 6.41 (dd, J = 8.3, 1.9 Hz, 1H), 6.35 (d, J = 1.9 Hz, 1H), 5.54 (br s, 1H), 4.57 (br s, 1H), 2.59–2.53 (m, 2H), 2.52–2.49 (m, 2H); MS (ESI) 423 $(M+H)^+$.

4.2.11. Dimethyl ether of dihydroptychantol A (15)

Pd/C 10% (250 mg) was added to a solution of **13** (2.25 g, 5.34 mmol) in ethyl acetate (150 mL). The suspension was stirred under H_2 for 24 h at room temperature. The reaction mixture was filtered, and the solution was concentrated to provide the

crude product that was recrystallized from ethanol to yield **15** (2.2 g, 96%) as a white solid; mp 202–203 °C. ^{1}H NMR (300 MHz, $CDCl_3$) δ 7.10 (t, J = 7.8 Hz, 1H), 6.92–6.85 (m, 6H), 6.82–6.70 (m, 4H), 6.33–6.21 (m, 3H), 3.93 (s, 3H), 3.80 (s, 3H), 2.97 (s, 4H), 2.64–2.57 (m, 2H), 2.53–2.46 (m, 2H); MS (ESI) 453 $(M+H)^+$.

4.2.12. Dihydroptychantol A (16)

A solution of boron tribromide (2.65 g, 10.61 mmol) in anhydrous CH_2Cl_2 (15 mL) was added dropwise to a stirred solution of **15** (0.6 g, 1.33 mmol) in anhydrous CH_2Cl_2 (15 mL) at −78 °C. The reaction mixture was stirred at −78 °C for 3 h, and then was allowed to warm up to room temperature within 12 h. The ice-cold water was added and the reaction mixture was stirred for 1 h. The solution was then diluted with CH_2Cl_2 (50 mL), washed with satd aq NaCl (20 mL × 3), and dried over sodium sulfate. The solution was concentrated, and the residue was purified by flash column chromatography (SiO_2), eluting with CH_2Cl_2 to yield **16** (0.3 g, 73%) as a grey solid; mp 165–167 °C. ^{1}H NMR (300 MHz, $CDCl_3$) δ 7.10 (t, J = 8.0 Hz, 1H), 6.94–6.88 (m, 5H), 6.86 (d, J = 8.4 Hz, 1H), 6.80 (d, J = 8.6 Hz, 1H), 6.73 (d, J = 3 Hz, 1H), 6.70 (dd, J = 8.0, 1.9 Hz, 1H), 6.64 (dd, J = 8.6, 3.0 Hz, 1H), 6.31–6.26 (m, 2H), 6.16 (d, J = 1.9 Hz, 1H), 5.56 (br s, 1H), 4.59 (br s, 1H), 3.00–2.94 (m, 4H), 2.61–2.56 (m, 2H), 2.50–2.44 (m, 2H); MS (ESI) 425 $(M+H)^+$.

4.2.13. 7-Hydroxyl-8-bromo derivative of demethyl ether of dihydroptychantol A (17)

N-Bromosuccinimide (149 mg, 0.83 mmol) was added to a suspension of **13** (250 mg, 0.56 mmol) in THF-H_2O (1:1) (12 mL) in three portions over 15 min at 0 °C. The reaction mixture was stirred vigorously at 0 °C for 0.5 h and then was allowed to warm up to 50 °C. After 5 h, the mixture was poured into 5% aq $Na_2S_2O_3$ (10 mL) and extracted with CH_2Cl_2 (25 mL × 3). The combined organic layer was then dried over sodium sulfate. The solution was concentrated, and the residue was purified by flash column chromatography (SiO_2), eluting with a 1:1 solution of petroleum ether–CH_2Cl_2 to afford **17** (186 mg, 61%) as a white solid; mp 216–218 °C. ^{1}H NMR (300 MHz, $CDCl_3$) δ 7.68 (d, J = 8.4 Hz, 1H), 7.28 (d, J = 8 Hz, 1H), 7.23–7.17 (m, 3H), 7.05 (s, 1H), 6.87–6.85 (m, 2H), 6.75 (dd, J = 8.8, 2.8 Hz, 1H), 6.66–6.58 (m, 2H), 6.46 (s, 1H), 6.29 (dd, J = 8.2, 2.0 Hz, 1H), 6.07 (s, 1H), 5.07 (d, J = 9.7 Hz, 1H), 5.00 (d, J = 9.7 Hz, 1H), 3.91 (s, 3H), 3.82 (s, 3H), 3.14 (br s, 1H), 2.71 (t, J = 8.3 Hz, 2H), 2.51–2.35 (m, 2H); ^{13}C NMR (75 MHz, $CDCl_3$) δ 158.5, 156.8, 155.4, 149.5, 147.2, 145.9, 139.9, 135.9, 134.7, 134.6, 130.2, 129.9, 126.8, 123.0, 122.5, 121.6, 121.4, 121.2, 117.2, 115.7, 115.1, 112.8, 112.5, 111.7, 79.0, 63.9, 56.1, 55.6, 37.1, 34.8; HRMS (ESI) calcd for $C_{30}H_{27}O_5Br$ 547.1115, found: 547.1106 $(M)^+$; MS (ESI) 529 $(M-H_2O)^+$.

4.2.14. 7-Keto-8-bromo derivative of demethyl ether of dihydroptychantol A (18)

A solution of anhydrous DMSO (47 μL, 0.66 mmol) in CH_2Cl_2 (5 mL) was added to a stirred solution of trifluoroacetic anhydride (69 μL, 0.5 mmol) in CH_2Cl_2 (10 mL) at −55 °C. After 30 min, a solution of **17** (180 mg, 0.33 mmol) in dry CH_2Cl_2 (15 mL) was added dropwise. The reaction mixture was stirred at −50 °C for 2 h. Triethylamine (143 μL, 0.99 mmol) was added slowly and the reaction mixture was then allowed to warm up to room temperature. After 0.5 h, the CH_2Cl_2 layer was washed with water (20 mL × 3) and dried over sodium sulfate. The solution was concentrated to provide a crude product that was purified by precipitating from CH_2Cl_2–hexane to afford **18** (167 mg, 93%) as a white solid; mp 244–246 °C. ^{1}H NMR (300 MHz, $CDCl_3$) δ 7.89 (d, J = 8.4 Hz, 1H), 7.66 (d, J = 8.7 Hz, 1H), 7.15–7.00 (m, 4H), 6.94 (d, J = 8.7 Hz, 1H), 6.88–6.82 (m, 4H), 6.77 (dd, J = 8.7, 3.0 Hz, 1H), 6.40 (s, 1H), 6.25 (d, J = 7.8 Hz, 1H), 5.83 (s, 1H), 3.93 (s, 3H), 3.82 (s, 3H), 2.70–2.52 (m, 2H), 2.49–2.37 (m, 2H); ^{13}C NMR (75 MHz, $CDCl_3$) δ 191.1, 159.7, 159.3, 157.2, 149.2, 147.4, 145.0, 139.3, 135.5, 134.2, 131.8, 131.2, 130.5, 130.4, 123.1, 123.0, 122.3, 122.1, 121.7, 117.2, 115.5, 115.4, 112.5, 112.3, 112.2, 56.93, 56.2, 55.6, 35.5, 31.6; HRMS (ESI) calcd for $C_{30}H_{25}O_5Br$ 545.0961, found: 545.0963 $(M)^+$; MS (ESI) 545 $(M)^+$.

4.2.15. 2-Amino-thiazole derivative of dimethyl ether of dihydroptychantol A (19)

A solution of **18** (80 mg, 0.15 mmol) and thiourea (17 mg, 0.23 mmol) in anhydrous DMF (15 mL) was stirred at 65 °C for 4 h. The reaction mixture was then diluted with CH_2Cl_2 (30 mL), washed with water (20 mL × 3), and dried over sodium sulfate. The solution was concentrated to provide a crude product that was purified by precipitating from CH_2Cl_2–hexane to afford **19** (63 mg, 83%) as a yellow solid. mp 270–272 °C; ^{1}H NMR (300 MHz, $CDCl_3$) δ 7.39 (d, J = 8.7 Hz, 2H), 7.18–7.01 (m, 4H), 6.93 (d, J = 8.7 Hz, 1H), 6.88–6.79 (m, 3H), 6.76–6.70 (m, 2H), 6.45–6.41 (m, 2H), 5.17 (br s, 2H), 3.95 (s, 3H), 3.82 (s, 3H), 2.60–2.56 (m, 2H), 2.55–2.51 (m, 2H); ^{13}C NMR (75 MHz, $CDCl_3$) δ 165.7, 158.8, 156.5, 155.8, 149.5, 149.4, 147.5, 145.4, 135.7, 134.8, 134.1, 131.0, 129.5, 122.4, 122.1, 122.0, 121.9, 121.3, 119.0, 116.4, 115.7, 112.4, 112.0, 111.9, 111.8, 56.2, 55.6, 37.7, 34.3; HRMS (ESI) calcd for $C_{31}H_{27}O_4N_2S$ 523.1686, found: 523.1673 $(M+H)^+$; MS (ESI) 523 $(M+H)^+$.

4.2.16. 2-Amino-thiazole derivative of dihydroptychantol A (20)

A solution of boron tribromide (213 mg, 0.88 mmol) in anhydrous CH_2Cl_2 (5 mL) was added dropwise to a stirred suspension of **19** (60 mg, 0.11 mmol) in anhydrous CH_2Cl_2 (10 mL) at −78 °C. The reaction mixture was stirred at −78 °C for 3 h, and the mixture was allowed to warm up to room temperature within 12 h. The ice-cold water was added, and the solution was stirred for 1 h. The solution was then diluted with CH_2Cl_2 (20 mL), washed with satd aq NaCl (20 mL × 3), and dried over sodium sulfate. The solution was concentrated to provide the crude product that was recrystallized from ethanol–H_2O to afford **20** (42 mg, 76%) as a yellow solid; mp 211–213 °C. ^{1}H NMR (600 MHz, DMSO-d_6) δ 9.37 (s, 1H), 9.28 (s, 1H), 7.31 (d, J = 8.4 Hz, 2H), 7.24 (s, 2H), 7.20 (t, J = 8.4 Hz, 1H), 7.03 (d, J = 8.4 Hz, 2H), 7.00 (dd, J = 7.2, 1.2 Hz, 1H), 6.83 (d, J = 8.4 Hz, 1H), 6.78 (d, J = 7.8 Hz, 1H), 6.73 (t, J = 3.0 Hz, 1H), 6.72 (d, J = 1.8 Hz, 1H), 6.64 (dd, J = 8.4, 3.0 Hz, 1H), 6.48 (t, J = 1.8 Hz, 1H), 6.30 (dd, J = 8.4, 2.4 Hz, 1H), 6.26 (d, J = 1.8 Hz, 1H), 2.44–2.42 (m, 2 H), 2.37–2.34 (m, 2H); ^{13}C NMR (150 MHz, DMSO-d_6) δ 166.5, 158.3, 155.0, 154.1, 147.5, 146.0, 144.6, 142.9, 134.9, 134.5, 132.3, 131.6, 130.7, 129.7, 122.2, 121.8, 121.6, 121.2, 118.2, 117.4, 116.5, 116.1, 115.7, 113.8, 110.6, 37.1, 33.4; HRMS (ESI) calcd for $C_{29}H_{23}O_4N_2S$ 495.1373, found: 495.1377 $(M+H)^+$; MS (ESI) 495 $(M+H)^+$.

4.2.17. 2-Hydrazino-thiazole derivative of dimethyl ether of dihydroptychantol A (21)

A solution of **18** (100 mg, 0.19 mmol) and thiosemicarbazide (26 mg, 0.29 mmol) in anhydrous DMF (20 mL) was stirred at 65 °C for 4 h. The reaction mixture was then diluted with CH_2Cl_2 (30 mL), washed with water (20 mL × 3), and dried over sodium sulfate. The solution was concentrated to provide a crude product that was purified by precipitating from CH_2Cl_2- hexane to afford **21** (57 mg, 56%) as a grey solid; mp 286–288 °C. ^{1}H NMR (300 MHz, DMSO-d_6) δ 7.26 (d, J = 8.4 Hz, 2H), 7.21 (d, J = 7.2 Hz, 1H), 7.15 (d, J = 7.8 Hz, 1H), 7.09 (d, J = 8.4 Hz, 2H), 7.00–6.93 (m, 3H), 6.86 (dd, J = 8.1, 1.8 Hz, 1H), 6.82 (dd, J = 8.7, 3.0 Hz, 1H), 6.33 (s, 1H), 6.29–6.25 (m, 2H), 2.48–2.41 (m, 4H); ^{13}C NMR (75 MHz, DMSO-d_6) δ 158.6, 156.5, 155.3, 149.5, 147.5, 147.4, 145.1, 145.0, 136.1, 135.5, 134.5, 134.6, 131.2, 130.1, 122.6, 122.5, 122.3, 122.1,

122.0, 118.4, 116.1, 115.8, 115.7, 113.2, 113.1, 113.0, 110.0, 56.2, 55.8, 37.6, 34.0; HRMS (ESI) calcd for $C_{31}H_{24}NO_4S$ 506.1420 $(M+H-NH_2NH_2)^+$, found: 506.1416 $(M+H-NH_2NH_2)^+$; MS (ESI) 506 $(M+H-NH_2NH_2)^+$.

4.2.18. 2-Hydrazino-thiazole derivative of dihydroptychantol A (22)

This compound was prepared from **21** by means of a procedure similar to that used for **20**. Yield 71%; mp 225–227 °C; ^1H NMR (600 MHz, DMSO-d_6) δ 7.25 (d, J = 8.4 Hz, 2H), 7.21 (t, J = 8.4 Hz, 1H), 7.14 (d, J = 8.4 Hz, 1H), 7.10 (d, J = 8.4 Hz, 2H), 6.81 (d, J = 9.0 Hz, 1H), 6.78 (d, J = 7.8 Hz, 1H), 6.74–6.72 (m, 2 H), 6.64 (dd, J = 8.4, 3.0 Hz, 1H), 6.31 (t, J = 1.8 Hz, 1H), 6.25 (dd, J = 8.4, 2.4 Hz, 1H), 6.22 (d, J = 1.8 Hz, 1H), 2.44–2.40 (m, 2 H), 2.39–2.34 (m, 2H); ^{13}C NMR (150 MHz, DMSO-d_6) δ 158.4, 155.2, 154.1, 150.9, 147.8, 146.1, 144.6, 143.1, 139.9, 134.9, 132.4, 131.1, 130.5, 129.5, 122.2, 122.0, 121.6, 121.4, 121.3, 117.6, 117.4, 116.6, 116.1, 115.6, 113.8, 112.9, 111.5, 37.2, 33.3; HRMS (ESI) calcd for $C_{29}H_{20}NO_4S$ 478.1107 $(M+H-NH_2NH_2)^+$, found: 478.1102 $(M+H-NH_2NH_2)^+$; MS (ESI) 510 $(M+H)^+$ and 478 $(M+H-NH_2NH_2)^+$.

4.3. Molecular modeling

The crystal structures of *P*-gp in complexation with two stereoisomers of cyclic hexapeptide inhibitors cyclic-*tris*-(*R*)-valineselenazole (QZ59-RRR) and cyclic-*tris*-(*S*)-valineselenazole (QZ59-SSS) were taken from Protein Data Bank (PDB code 3G60 and 3G61).[40] Hydrogens were added and minimized using the Tripos force field and Pullman charges. Modeled analogues were constructed in SYBYL 8.0,[41] and energy was minimized with the Tripos force field and Gasteiger-Hückel charges. Docking analogues into three different binding sties of *P*-gp was performed using GOLD program. For each of the genetic algorithm (GA) runs, a maximum number of 100,000 GA operations were performed on a single population of 100 individuals. Operator weights for crossover, mutation, and migration were set to 95, 95, and 10, respectively, which are the standard default settings recommended by the authors. The maximum distance between hydrogen donors and fitting points was set to 3.5 Å, and the cutoff value for van der Waals was 4.0. After docking, the best docked conformation of compound **19** was merged into the ligand-free protein. The new ligand–protein complex was subsequently subjected to energy minimization using Tripos force field with Pullman charges. During the energy minimization, the structure of the compound **19** and a surrounding 6 Å sphere were allowed to move, while the structures of the remaining protein were frozen. The energy minimization was performed using the Powell method with a 0.05 kcal/(mol Å) energy gradient convergence criterion and a distance-dependent dielectric function.

4.4. Biological evaluation

4.4.1. Cell culture

KB, KB/VCR, K562, and K562/A02 cells were cultured in RPMI 1640 medium (HyClone) supplemented with 10% fetal bovine serum (HyClone). The cells were maintained in 5% CO_2 at 37 °C until reaching approximately 50–70% confluence, and then treated with different amounts of chemicals. DMSO was used as a control vehicle.

4.4.2. Cytotoxicity and multidrug resistance reversal assay

The cytotoxicity of the tested compounds was evaluated in KB, KB/VCR, K562, and K562/A02 cells by the MTT assay. These four kinds of cells were propagated in 24-well culture plates and grown under the conditions described above. The cells were then treated with vehicle and tested compound alone for further 48 h. Cell growth response to the chemicals was detected by measuring the absorbance of formazan crystals produced by living cultured cells at 490 nm. Three replicates were used for each treatment and the assay was repeated at least thrice.

The multidrug resistance reversal ability of these compounds to potentiate adriamycin and vincristine cytotoxicity was evaluated in K562/A02 cells and in KB/VCR cells, respectively, by the MTT assay described above. The cells were treated with vehicle and tested compound combined with desired concentrations of chemicals. ID_{50} values for all tested compounds were calculated from plotted results using untreated cells as 100%. The reversal fold (RF) values, as potency of reversal, were obtained from fitting the data to RF = ID_{50} of cytotoxic drug alone/ID_{50} of cytotoxic drug in the presence of the test drugs.

Acknowledgments

This work was supported by grant from the *National Natural Science Foundation* (*NNSF*) of China (No. 30730109). S.B. wishes to thank Dr. Mark Cushman and his research group (Purdue University, USA) for assistance and insight.

References and notes

1. Teodori, E.; Dei, S.; Scapecchi, S.; Gualtieri, F. *Farmaco* **2002**, *57*, 385.
2. Krishna, R.; Mayer, L. D. *Eur. J. Pharmacol. Sci.* **2000**, *11*, 265.
3. Gottesmann, M. M.; Hrycyna, C. A.; Schoenlein, P. V.; Germann, U. A.; Pastan, I. *Annu. Rev. Genet.* **1995**, *29*, 607.
4. Cole, S. P. C.; Deeley, R. G. *Bioassays* **1998**, *20*, 931.
5. Grant, C. E.; Valdimarsson, G.; Hipfner, D. R.; Almquist, K. C.; Cole, S. P.; Deeley, R. G. *Cancer Res.* **1994**, *54*, 357.
6. Kruh, G. D.; Chan, A.; Myers, K.; Gaughan, K.; Miki, T.; Aaronson, S. A. *Cancer Res.* **1994**, *54*, 1649.
7. Kuwano, M.; Toh, S.; Uchiumi, T.; Takano, H.; Kohno, K.; Wada, M. *Anti-Cancer Drug Des.* **1999**, *14*, 123.
8. Szakács, G.; Paterson, J.; Ludwig, J.; Genthe, C.; Gottesman, M. *Nat. Rev. Drug Disc.* **2006**, *5*, 219.
9. Zinsmeister, H. D.; Becker, H.; Eicher, T.; Mues, R. *Naturwiss. Rundschau.* **1994**, *47*, 131.
10. Asakawa, Y. *Phytochemistry* **2001**, *56*, 297.
11. Jochen, M. S.; Elaine, J. B.; Stephen, D. L.; Nigel, B. P. *Tetrahedron* **2002**, *58*, 7875.
12. Asakawa, Y.; Toyota, M.; Taira, Z.; Takemoto, T. *J. Org. Chem.* **1983**, *48*, 2164.
13. Hioki, H.; Shima, N.; Kawaguchi, K.; Harada, K.; Kubo, M.; Esumi, T.; Nishimaki-Mogami, T.; Sawada, J.-I.; Hashimoto, T.; Asakawa, Y.; Fukuyama, Y. *Bioorg. Med. Chem. Lett.* **2009**, *19*, 738.
14. Suzuki, T.; Tamehiro, N.; Sato, Y.; Kobayashi, T.; Ishii-Watabe, A.; Shinozaki, Y.; Nishimaki-Mogami, T.; Hashimoto, T.; Asakawa, Y.; Inoue, K.; Ohno, Y.; Yamaguchi, T.; Kawanishi, T. *J. Pharmacol. Sci.* **2008**, *107*, 285.
15. Asakawa, Y. *Curr. Pharm. Des.* **2008**, *14*, 3067.
16. Scher, J. M.; Burgess, E. J.; Lorimer, S. D.; Perry, N. B. *Tetrahedron* **2002**, *58*, 7875.
17. Asakawa, Y.; Toyota, M.; Taira, Z.; Takemoto, T. *J. Org. Chem.* **1983**, *48*, 2164.
18. Xie, C.; Lou, H. *Chem. Biodiversity* **2009**, *6*, 303.
19. Shi, Y. Q.; Zhu, C. J.; Yuan, H. Q.; Li, B. Q.; Gao, J.; Qu, X. J.; Sun, B.; Cheng, Y. N.; Li, S.; Li, X.; Lou, H. X. *Cancer Lett.* **2009**, *276*, 160.
20. Morita, H.; Tomizawa, Y.; Tsuchiya, T.; Hirasawa, Y.; Hashimoto, T.; Asakawa, Y. *Bioorg. Med. Chem. Lett.* **2009**, *19*, 493.
21. Shi, Y. Q.; Qu, X. J.; Liao, Y. X.; Xie, C. F.; Cheng, Y. N.; Li, S.; Lou, H. X. *Eur. J. Pharmacol.* **2008**, *584*, 66.
22. Qu, J.; Xie, C.; Guo, H.; Yu, W.; Lou, H. *Phytochemistry* **2007**, *68*, 1767.
23. Li, X.; Sun, B.; Zhu, C. J.; Yuan, H. Q.; Shi, Y. Q.; Gao, J.; Li, S. J.; Lou, H. X. *Toxicol. In vitro* **2008**, *23*, 29.
24. Jin, Z. *Nat. Prod. Rep.* **2005**, *22*, 196.
25. Morris, L. A.; Bosch, J. J. K. v. d.; Versluis, K.; Thompson, G. S.; Jaspars, M. *Tetrahedron* **2000**, *56*, 8345.
26. Bazargan, L.; Fouladdel, S.; Shafiee, A.; Amini, M.; Ghaffari, S. M.; Azizi, E. *Cell Biol. Toxicol.* **2008**, *24*, 165.
27. Ogino, J.; Moore, R. E.; Patterson, G. M. L.; Smith, C. D. *J. Nat. Prod.* **1996**, *59*, 581.
28. Simoni, D.; Grisolia, G.; Giannini, G.; Roberti, M.; Rondanin, R.; Piccagli, L.; Baruchello, R.; Rossi, M.; Romagnoli, R.; Invidiata, E. P.; Grimaudo, S.; Jung, M. K.; Hamel, E.; Gebbia, N.; Crosta, L.; Abbadessa, V.; Cristina, A. D.; Dusonchet, L.; Meli, M.; Tolomeo, M. *J. Med. Chem.* **2005**, *48*, 723.
29. Tirado, R. J.; Gandour, R. D. *Chem. Ber.* **1984**, *17*, 62.
30. Boden, R. M. *Synthesis.* **1975**, 784.
31. Eicher, T.; Fey, S.; Puhl, W.; Büchel, E.; Speicher, A. *Eur. J. Org. Chem.* **1998**, *5*, 877.
32. Hanessian, S.; Huang, G.; Chenel, C.; Machaalani, R.; Loiseleur, O. *J. Org. Chem.* **2005**, *70*, 6721.
33. Appell, R. B.; Duguid, R. *Org. Process Res. Dev.* **2000**, *4*, 172.

34. Ohsumi, K.; Hatanaka, T.; Fujita, K.; Nakagawa, R.; Fukuda, Y.; Nihei, Y.; Morinaga, Y.; Akiyama, Y.; Tsuji, T. *Bioorg. Med. Chem. Lett.* **1998**, *8*, 3153.
35. Aller, S. G.; Yu, J.; Ward, A.; Weng, Y.; Chittaboina, S.; Zhuo, R.; Harrell, P. M.; Trinh, Y. T.; Zhang, Q.; Urbatsch, I. L.; Chang, G. *Science* **2009**, *323*, 1718.
36. Verdonk, M. L.; Cole, J. C.; Hartshorn, M. J.; Murray, C. W.; Taylor, R. D. *Proteins* **2003**, *52*, 609.
37. Jones, G.; Willett, P.; Glen, R. C.; Leach, A. R.; Taylor, R. *J. Mol. Biol.* **1997**, *267*, 727.
38. Wang, R.; Lu, Y.; Wang, S. *J. Med. Chem.* **2003**, *46*, 2287.
39. Nishio, M.; Hirota, M. *Tetrahedron* **1989**, *45*, 7201.
40. www.rcsb.org.
41. *SYBYL 8.0 for Linux*; Tripos, Inc.: 2007. 1699 South Hanley Rd., St. Louis, MO 63144-2917, USA.